

See discussions, stats, and author profiles for this publication at: <https://www.researchgate.net/publication/231665871>

Effect of Penetration Enhancers on the Dynamic Behavior of Phosphatidylcholine Headgroups in Liposomes

ARTICLE *in* THE JOURNAL OF PHYSICAL CHEMISTRY B · JANUARY 2000

Impact Factor: 3.3 · DOI: 10.1021/jp9925482

CITATIONS

18

READS

12

7 AUTHORS, INCLUDING:



Irina Ermolina

De Montfort University

51 PUBLICATIONS 866 CITATIONS

SEE PROFILE



Yaroslav Ryabov

n/a

60 PUBLICATIONS 1,013 CITATIONS

SEE PROFILE



Raoul Rashid Nigmatullin

Kazan National Research Technical University

185 PUBLICATIONS 2,057 CITATIONS

SEE PROFILE



Yuri D Feldman

Hebrew University of Jerusalem

187 PUBLICATIONS 2,832 CITATIONS

SEE PROFILE

Effect of Penetration Enhancers on the Dynamic Behavior of Phosphatidylcholine Headgroups in Liposomes

I. Ermolina,[†] G. Smith,[§] Ya. Ryabov,[‡] A. Puzenko,[†] Yu. Polevaya,[†] R. Nigmatullin,[‡] and Yu. Feldman^{*,†}

Department of Applied Physics, Hebrew University of Jerusalem, 91904 Jerusalem, Israel, Department of Theoretical Physics, Kazan State University, Kazan, Russia, and School of Pharmacy and Pharmaceutical Sciences, De Montfort University, Leicester, U.K.

Received: July 23, 1999; In Final Form: November 15, 1999

The results of a time-domain dielectric spectroscopy (TDDS) study of the effect of two skin penetration modulators on phosphatidylcholine (PC) bilayer vesicles are presented. The complex dielectric permittivity spectra of PC vesicle suspensions were described as the sum of two processes: the interfacial polarization of the bilayer and the reorientation of the zwitterionic PC headgroups in a plane approximately tangential to the bilayer surface. The influence of two additives (Azone and Transcutol) on the structure and dynamic behavior of PC headgroups of the bilayer vesicles was analyzed in terms of the interconnection of the dielectric spectra Cole–Davidson parameter, β , and the correlation factor, g , of the dielectric relaxation Kirkwood cell model. Analytically, these parameters are connected in the proposed model via the spatial distribution of headgroup dipole nonhomogeneities. In terms of the physical modulation of the polar surface phase, it appears that these additives can behave either as enhancers or as retarders. Their activity in this respect depends on the concentration of additive and temperature.

I. Introduction

It is well-known that the main barrier to skin permeation is the complex array of lipids, which exist as structured bilayers within the stratum corneum.¹ Permeation of solutes through this barrier can be enhanced or retarded through the use of barrier function modulators,² such as oleic acid and Azone (i.e., 1-dodecylazacycloheptan-2-one or laurocapram), or solvents, such as Transcutol (diethylene glycol monoethyl ether). The exact mechanisms of barrier function modulators remain unclear, although there is a large body of evidence to suggest that most skin penetration modulators act by increasing the fluidity of the hydrophobic regions of the intercellular liquids,^{3–5} whereas others may exert their effect by increasing the partitioning or solubility of permeants within the stratum corneum.^{6,7} The former mechanism is thought to result from an interaction between the penetration modulator and the polar headgroup region, leading to disruption in the packing of the acyl chains and increased fluidity. However, because of the lack of suitable methods, much less is known about the direct effect of this interaction on the headgroup region itself. To examine this aspect, one needs to be able to probe the polar region of lipid bilayers, ideally by some noninvasive method. To this end, this paper has explored the use of high-frequency (200 kHz to 3 GHz) time-domain dielectric spectroscopy in the investigation of the polar region of a model membrane system, i.e., the zwitterionic headgroup of phosphatidylcholine (PC) bilayer vesicles.

In the high-frequency dielectric analysis of PC vesicles, the zwitterionic headgroups are assumed to polarize by rotating in

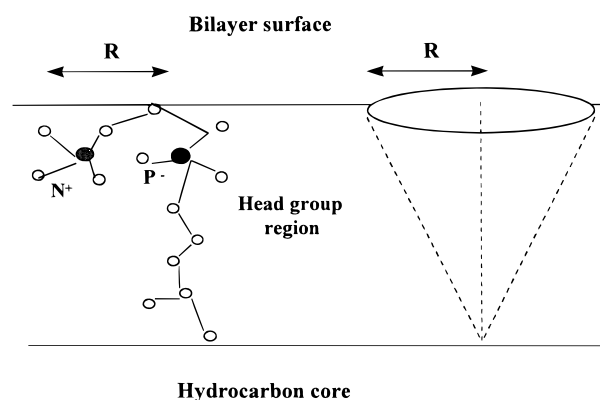


Figure 1. Schematic presentation of the orientational mobility of the zwitterionic headgroup of PC bilayer.

a manner describing a cone with an axis normal to the membrane (Figure 1). Relaxation times for this process have been observed between 0.5 and 8 ns (corresponding to a frequency range of 20–300 MHz).^{8–12} The dynamics of reorientation depends both on the immediate environment of the headgroups and on the long-range order in the system, and therefore, the dielectric relaxation time is sensitive to parameters such as membrane fluidity and molecular packing.

The authors recognize that PC is not present naturally in the stratum corneum, but similar studies by dielectric relaxation spectroscopy on indigenous lipids of the stratum corneum would be impossible, owing to the absence of lipids with a dipolar headgroup. (The stratum corneum consists of ~40% ceramides, ~40% cholesterol, and ~10% fatty acids.¹³) Nevertheless, this type of study is still considered to be of value because the results will highlight any nonspecific effects that penetration modulators and solvents exert on lipid bilayer surfaces.

* To whom correspondences should be addressed. Phone: +972-2-6586187. E-mail: Yurif@vms.huji.ac.il. Fax: +972-2-5663878.

[†] Hebrew University of Jerusalem.

[§] De Montfort University.

[‡] Kazan State University.

TABLE 1: Composition of the Egg Lecithin (Lipid Products), the Gel–Liquid Crystalline Transition Temperature,¹⁴ T_c , for Pure Lipid Species, and Saturation of Some of Them

lipid species	composition, %	T_c , °C	saturation, %
C16:0	32.1	41	44.8
C18:0	11.7	54	
C16:1	2.1	−36	
C18:1	36.2	−20	
C18:2	12.5	<−20	55.2
C20:4	5.5	<−20	

II. Materials and Methods

2.1. Preparation of Liposome Suspensions. Small, primarily unilamellar liposomes (10% w/v lipid) were prepared from solutions of grade I egg lecithin (Lipid Products) and additive (0, 5, 10, and 20 mol % Transcutol or Azone) in chloroform/methanol (6:1 by volume). A dry film of the material was formed on the bottom of a 15 mL flat-bottomed glass sample jar by evaporation of the solvent under partial vacuum. The dry film was then sparged with nitrogen for 5 min before hydrating for 20 min in distilled water at 60 °C. The liposomes formed were then probe-sonicated for 4 min.

The composition of the egg lecithin (Lipid Products), the gel–liquid crystalline transition temperature,¹⁴ T_c , for the pure lipid species, and the degree of saturation for some of these lipids are presented in Table 1.

2.2. Measurement of Dielectric Parameters. The dielectric properties of liposome suspensions were determined by a commercial time-domain dielectric spectrometer (TDS), manufactured by Dipole TDS, Jerusalem.¹⁵ This spectrometer determines dielectric properties of materials by measuring the response of a sample to a rapidly increasing step voltage (i.e., with a short rise time).

In the framework of the lumped capacitance approximation, the complex dielectric permittivity is written as

$$\epsilon^*(\omega) = \frac{1}{i\omega C_0} \frac{L[I(t)]}{L[V(t)]} \quad (1)$$

where $I(t)$ is the current flowing through the sample, $V(t)$ is the voltage applied to the sample, L is the operator of the Laplace transform, and C_0 is the capacitance of the empty sample cell that terminates the end of the coaxial line (the capacitance of the empty cell is 0.2 pF).

A small sample (about 150 μ L) of each liposome suspension was injected into the sample cell, and the time-domain response of the sample was determined from the accumulation of 25 600 individual scans. Nonuniform sampling of the time window (4.4 μ s) for each pulse enables the generation of spectra in the frequency range from 200 kHz to 3 GHz. Measurements were taken as a function of increasing temperature from 5 to 40 °C at intervals of 5 °C. The measurement accuracy of the dielectric permittivity and loss was better than 5%.¹⁵ The accuracy of fitting (i.e., the mean square deviation) was less than 10^{-3} .

III. Results

The Cole–Cole diagram of a typical complex dielectric permittivity spectrum is presented in Figure 2. Analysis of all spectra has shown that the best fitting was obtained by using the function comprising two processes: a Debye process and a

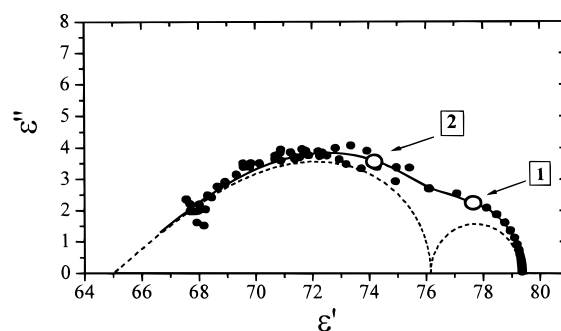


Figure 2. Cole–Cole diagram of the complex dielectric permittivity for liposome suspension without additives at 15 °C. Solid line is a fitting line by using eq 2. Dashed lines represent two relaxation processes, corresponding to eq 2. Parameters of processes are the following: $\epsilon_{\text{inf}} = 65$, $\tau_1 = 59.7$ ns, $\Delta\epsilon_1 = 3.146$, $\tau_2 = 8.6$ ns, $\Delta\epsilon_2 = 11.15$, and $\beta = 0.42$. Open circles show the dielectric permittivities and losses at the characteristic frequencies corresponding to the relaxation times of the first and second processes.

Cole–Davidson process:

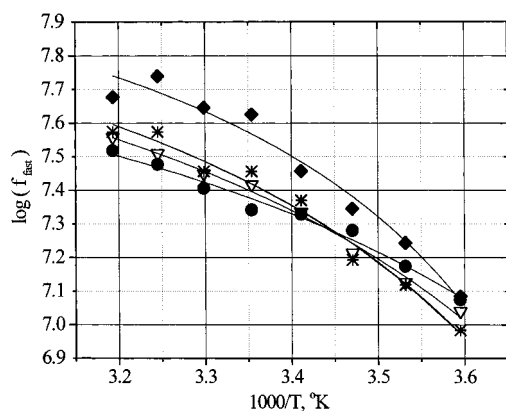
$$\epsilon^*(\omega) = \epsilon_{\infty} + \frac{\Delta\epsilon_1}{1 + j\omega\tau_1} + \frac{\Delta\epsilon_2}{(1 + j\omega\tau_2)^{\beta}} \quad (2)$$

where τ_i and $\Delta\epsilon_i$ are the relaxation time and relaxation strength of the i process, ω is angular frequency, ϵ_{∞} is the high-frequency limit of the dielectric permittivity, and β is the Cole–Davidson parameter.

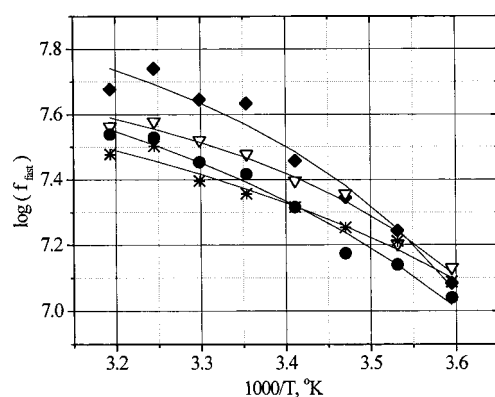
The relaxation time of the slow process (subscript 1 in eq 2) for all samples was in the range 50–70 ns and practically independent of temperature. The dielectric strength of this process was about 10 and had a weak dependence on temperature.

The characteristic frequencies (i.e., the reciprocal of the relaxation time) for the fast process (subscript 2 in eq 2) as a function of $1000/T$ are presented in Figure 3 for PC vesicle suspensions with Azone and Transcutol additives. The temperature dependence of the characteristic frequency is non-Arrhenius in behavior and can be fitted by the Vogel–Fulcher–Tammann (VFT) function.¹⁶ The temperature dependence of the dielectric strength, $\Delta\epsilon$, and the Cole–Davidson parameter, β , are presented in Figures 4 and 5, respectively. The dielectric strength decreases with increasing temperature for both sets of samples. At temperatures below 20 °C, the dielectric strength of the relaxation decreases with increasing amounts of Transcutol. The exception to this tendency was the sample with 20 mol % Transcutol. At temperatures above 20 °C, the dielectric strength of the relaxation increases with increasing amounts of Transcutol. The dielectric strength for samples with Azone was affected much less by the concentration of additive. Again, the exception was the sample with 20 mol % additive, in which the dielectric strength increases at temperatures above 20 °C. The parameter β changes from ~ 0.4 to ~ 0.8 as the temperature is increased from 5 to 35 °C for both additives.

It has been shown that the dielectric behavior of liposome suspensions is characterized by four dispersions.^{17,18} They are usually ascribed to the following mechanisms: the tangential movement of counterions at the vesicle surface (1 kHz to 1 MHz);¹⁷ interfacial polarization (1–100 MHz);¹⁷ the rotational diffusive motion of the lipid headgroup (30–500 MHz);^{18,19} the reorientation of the water of hydration (>1 GHz).^{18,20} The relaxation time of the fastest process is outside the experimental frequency range of this study. For the slowest process, the characteristic frequency for the liposome vesicles was estimated



a.



b.

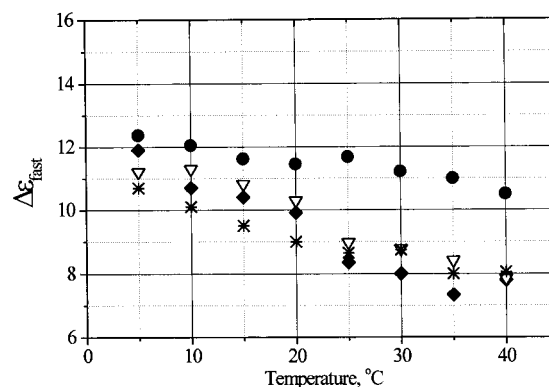
Figure 3. Characteristic frequency of the fast process vs inverse temperature for different amounts of Azone (a) and Transcutol (b): (◆) 0%; (▽) 5%; (*) 10%; (●) 20%.

from an expression for counterion relaxation.¹⁷ It was found that this characteristic frequency is less than 40 kHz and therefore also outside the experimental frequency range used in this study.

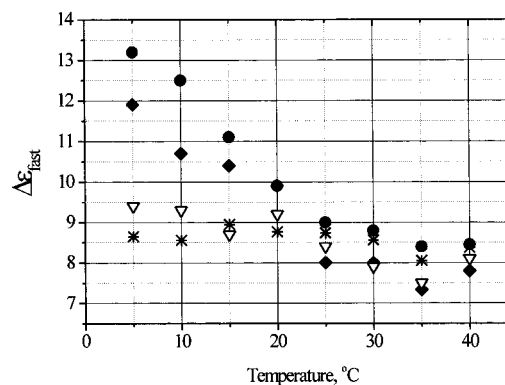
It is therefore concluded that the slow Debye-type dispersion observed in this study (see τ_1 , $\Delta\epsilon_1$, or eq 2) relates to the interfacial charging of the vesicle bilayers through the intra- and extravescule solution resistances. Numerical estimation of the relaxation time for interfacial polarization of lipid vesicles, using the Maxwell–Wagner and single-shell models,²¹ gave a relaxation time between 50 and 80 ns that is in good agreement with the experimental data. Moreover, it was observed that there was no essential temperature dependence of the relaxation time τ_1 , an observation that is typical for Maxwell–Wagner processes.²² The fast process (subscript 2, eq 2) is thought to result from the reorientation of the PC headgroups in the plane of the bilayer surface¹⁰ and forms the main subject of this paper.

IV. Discussion

4.1. Structural Model for PC Headgroups and Short-Range Correlation. Small unilamellar liposomes are approximately spherical vesicular structures with a shell that is structured from a bimolecular leaflet of phosphatidylcholine. The polar end of the PC molecule consists of a zwitterionic



a.



b.

Figure 4. Temperature dependence of the dielectric strength of the fast relaxation process in the presence of Azone (a) and Transcutol (b): (◆) 0%; (▽) 5%; (*) 10%; (●) 20%.

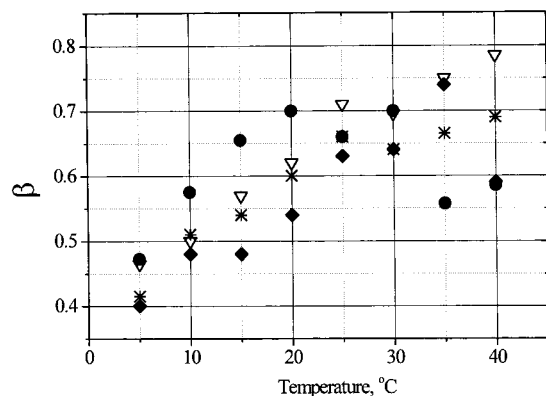
headgroup that sits at the bilayer–water interface. The headgroup is assumed to rotate in a manner that describes a cone centered on the bilayer normal (Figure 1). The hydrophobic end of the molecule consists of two acyl chains that form the core of the bilayer. To describe the structural behavior of the headgroups in PC bilayer vesicles, we have put forward a model based on a hexagonal face-centered unit cell (Figure 6).

The dipole moment of a single PC headgroup, μ , results from the unit charges at the P and N atoms being separated by a distance of approximately 4.5 Å. We have supposed that the headgroups are oriented parallel to the bilayer surface,²³ though a slight out-of-plane displacement of approximately 5° has been included to account for the potential hydrophobic displacement of the choline group ($-\text{N}(\text{CH}_3)_3$) below the plane of the bilayer. The vector of the dipole moment, μ , can therefore be resolved into two components: one component, $\mu \sin \gamma$, is parallel (i.e., tangential) to the bilayer surface and the other, $\mu \cos \gamma$, is perpendicular (i.e., normal) to the bilayer surface.

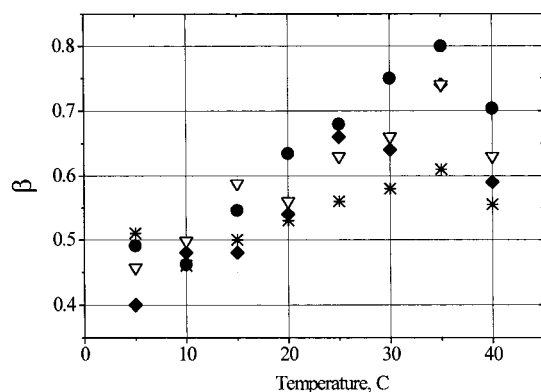
The spatial distribution of dipole correlations over the short distance and time scales can be described by the following expression for the well-known Kirkwood correlation factor, g :²¹

$$g = 1 + (N - 1)\langle \cos \varphi \rangle \quad (3)$$

In eq 3, N is the number of dipoles in a unit Kirkwood cell and $\langle \cos \varphi \rangle$ describes the average cosine of all the angles, φ , between each dipole and its neighbors in the Kirkwood cell. The parameter g can be evaluated from experimental dielectric



a.



b.

Figure 5. Temperature dependence of Cole–Davidson parameter β for different amounts of Azone (a) and Transcutol (b): (◆) 0%; (▽) 5%; (*) 10%; (●) 20%.

spectra by equation²⁴

$$g = \frac{9kT\epsilon_0}{\mu^2 N_a} \frac{(\Delta\epsilon_2)(2\Delta\epsilon_2 - \epsilon_{l\infty})}{(\Delta\epsilon_2 - \epsilon_{l\infty})(\epsilon_{l\infty} + 2)^2} \quad (4)$$

In eq 4, μ is the value of the dipole moment of the PC headgroup, T is the temperature, k is the Boltzman constant, N_a is the Avogadro number, $\Delta\epsilon_2$ is the dielectric strength of the fast process, $\epsilon_{l\infty}$ is the dielectric permittivity of the liposome bilayer at high frequencies, and ϵ_0 is the dielectric permittivity of vacuum. We note that $\epsilon_{l\infty}$ is not equal to ϵ_∞ in eq 2 for a mixture of lecithin and water. Moreover, this parameter is probably different from the analogous parameter for nonstructured pure lecithin. The procedure for numerical estimation of $\epsilon_{l\infty}$ is presented later in the paper. It should be mentioned that eq 4 was derived for the pure polar liquid in the bulk phase. Nevertheless, we use this equation for the lecithin bilayers as a first approximation.

In the framework of our model, the Kirkwood correlation factor, g , can be presented by the sum of two components. These components are related to the behavior of perpendicular and parallel components of the dipole moments of the PC headgroups:

$$g = g_1 \sin^2 \gamma + g_2 \cos^2 \gamma \quad (5)$$

In eq 5, g_1 is the planar correlation factor of the parallel dipole

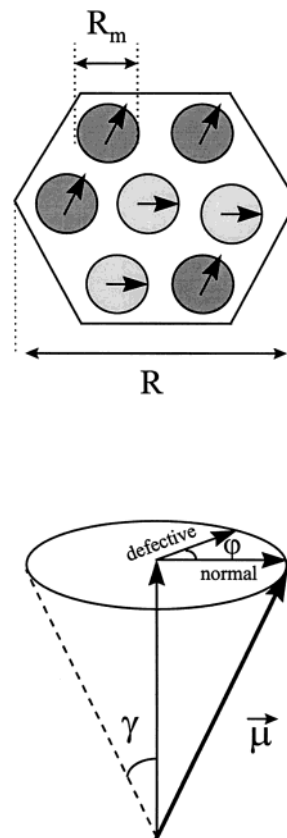


Figure 6. Schematic showing the Kirkwood unit cell for PC head dipole moments. Here, φ is angle between “normal” and “defective” dipole moments, γ is the angle between the dipole moment and the perpendicular to the bilayer surface.

moments of the PC headgroups and g_2 is the planar correlation factor of perpendicular dipole moments of the PC headgroups. Both of these components have to obey eq 3.

The perpendicular components of the dipole moments are completely correlated because they are parallel to each other. In this case, $\langle \cos \varphi \rangle = 1$ in eq 3, and the correlation factor for the perpendicular components, g_2 , can be taken to be equal to the number of dipoles in the unit cell, i.e.,

$$g_2 = N = 7 \quad (6)$$

The tangential components of the dipole moment are thought to rotate as shown in Figure 1. While it is assumed that the rotation rate for all these dipoles is the same, it is recognized that there will be phase differences between the tangential rotation of individual dipoles in the surface population of a liposome vesicle, and therefore, the tangential components will be at least partially correlated. In the extreme case, when the phase shift between the rotation of all the dipoles is purely random (i.e., the random phase shift is distributed equally over the range from 0 to 2π), a correlation factor of zero would result, and the rotation is said to completely noncorrelated. At the other extreme, when the rotation of the headgroups is completely correlated, the phase shift between nearest-neighboring dipoles in the Kirkwood cell is zero (i.e., the rotation of the parallel components is synphase). The correlation factor would then be equal to the number of PC headgroups in the unit cell ($N = 7$). In reality, there will be a distribution of phase shifts between neighboring PC headgroups. However, for the purpose of simplification we have developed a model that considers an intermediate situation in which there are two populations of unit dipoles and their rotation occurs relative to each other with a

phase shift φ . One population of headgroups is described as “normal” (they have a phase shift of zero), whereas the other population is described as “defective” (they have a phase shift of φ). The correlation factor g_1 is described by eq 3 where φ is the angle between the tangential dipole moment components of the “normal” and “defective” headgroups in the plane of the Kirkwood cell. The minimum energy conformation of the PC unit cell corresponds to the parallel or antiparallel positions of the dipole moments, and therefore, it is convenient to suppose that the angle φ (describing the phase shift of the “defective” dipoles in the unit cell) should be equal to 180° .²⁵

4.2. Interconnection between Short- and Long-Range Correlation of PC Headgroups. Experimental studies on egg phosphatidylcholine bilayer vesicles have shown that the temperature dependencies are manifested for both the structural parameters ($\Delta\epsilon$ and consequently g) and dynamic parameters (τ and β) of the dielectric relaxation in the range 5–40 °C. As we noted in section 4.1, the parameter g describes the short-range interactions in the framework of the Kirkwood unit cell. The β parameter, however, relates to the dielectric response from structural units on all scales, including the macroscopic scale. Hence, the experimentally observed temperature-dependent behaviors of both parameters, g and β , indicate the existence of an interconnection between short- and long-range correlation of PC headgroups.

We believe that this interconnection exists because the specific spatial distribution of the nonhomogenities (defects) in the sample is the same over all ranges of scale. To determine the analytical relationship between g and β , we will consider two approaches: a “classical” approach and a fractal approach.

Classical Approach. The classical approach is based on the model of an effectively continuous medium and enables the calculation of the Kirkwood correlation factor from experimental spectra by using eq 4. In this approach, the surfaces of the liposomes are assumed to exist as close-packed Kirkwood cells. Each cell has an effective dipole moment, which is defined by the value of the dipole moment of an individual PC headgroup and the interactions between the headgroups within the framework of the Kirkwood cell. To evaluate the number of defects n in the Kirkwood cell, we shall consider two situations where either a “normal” or a “defective” dipole is located at the center of the unit cell, with probabilities P_n or P_d , respectively. If N is the total number of dipoles in the cell, then for these two cases,

$$\begin{aligned} P_n &= \frac{N-n}{N} \\ P_d &= \frac{n}{N} \end{aligned} \quad (7)$$

and the mean cosines of the angle φ (see eq 3) are equal to

$$\begin{aligned} \langle \cos \varphi \rangle_n &= \frac{n \cos \varphi + N - n - 1}{N - 1} \\ \langle \cos \varphi \rangle_d &= \frac{(N - n) \cos \varphi + n - 1}{N - 1} \end{aligned} \quad (8)$$

In total,

$$\langle \cos \varphi \rangle = P_n \langle \cos \varphi \rangle_n + P_d \langle \cos \varphi \rangle_d \quad (9)$$

Substitution of eqs 7 and 8 into eq 9 then allows the determination of the mean cosine of φ ($\langle \cos \varphi \rangle$).

$$\langle \cos \varphi \rangle = 1 - \frac{2n(N-n)}{N(N-1)}(1 - \cos \varphi) \quad (10)$$

The number of defects, n , in the Kirkwood cell can then be obtained by solving eq 10, where angle φ is assumed to equal 180° and $\langle \cos \varphi \rangle$ is calculated from

$$\langle \cos \varphi \rangle = \frac{g_1}{1 + (N-1)} \quad (11)$$

where g_1 is obtain from eqs 4–6.

To calculate n from the experimental data, it is necessary to know the value of $\epsilon_{l\infty}$ (see eq 4), which is not measured directly. In an earlier publication²⁶ this parameter was estimated as $4.6 < \epsilon_{l\infty} < 5.6$. The value 5.0 can therefore be accepted as a first approximation for the liposome vesicle. Another way to obtain $\epsilon_{l\infty}$ is to calculate it by using the Kraszewski mixture formula.²⁷ This formula should apply to that region in the high-frequency part of the vesicle suspension spectrum where the dielectric permittivity of the water phase is still equal to the static value. Our estimation has shown that $\epsilon_{l\infty}$ was very sensitive to a small error in the volume fraction of lecithin or in the measurement of the static permittivity of water. Nevertheless, it was still possible to obtain the value of $\epsilon_{l\infty}$ with reasonable accuracy. In this study, therefore, $\epsilon_{l\infty}$ was taken to equal 7.

Fractal Approach. This approach is based on the assumption that the distribution of defects on the liposome surface is fractal in nature on all scales, from the size of the elementary dipoles, R_m , to the macroscopic size of sample R_{\max} . Central to the fractal approach is the idea that the connection among the fractal dimension D , the Euclidean dimension d , and the parameter of Cole–Davidson, β , is given by²⁸

$$D = d\beta \quad (12)$$

To reconcile the fractal and classical models, we have to assume that the average number of defects n for the Kirkwood model is equal to the average number of defects $\langle n_f \rangle$ for the fractal model on the scale of the Kirkwood cell, R , i.e.,

$$n(T, \epsilon_{l\infty}) = \langle n_f(T) \rangle \quad (13)$$

We are suggesting that the parameter n is a significant characteristic defining the order–disorder in the bilayer surface and, as such, may be related to the permeability of the bilayer surface to solutes.

A statistical fractal approach was developed for the description of the number of defects $\langle n_f(T) \rangle$ in eq 13 (see Appendix). By use of the assumption in eq 12 for eq A11, it is possible to obtain the average number of defects in the unit Kirkwood cell of size R :

$$\langle n_f(T) \rangle = \Omega \frac{\left(\frac{R_m}{R}\right)^{-b} 1 - \left(\frac{R_m}{R}\right)^{b[1-\beta(T)]+1}}{1 - \frac{R_m}{R} b[1-\beta(T)] + 1} \quad (14)$$

It is necessary to remark that with the help of this model one can estimate the average number of elementary defects in a unit cell with an accuracy of up to a dimensionless geometrical shape factor Ω .

The comparison of the models presented above can be performed through an estimation of the number of defects. We have made a number of assumptions in order to calculate the number of defects in the Kirkwood unit cell. The assumptions

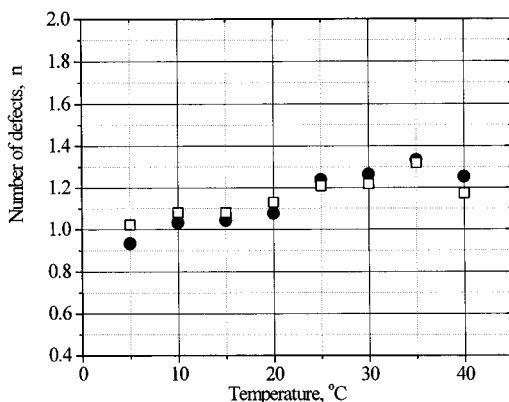


Figure 7. Temperature dependencies of number of defects calculated by classical (●) and fractal (□) ($\Omega = 0.28$) models.

in the calculation are as follows: (i) the number of dipoles in a unit cell is given by $N = 7$; (ii) the dielectric permittivity of a bilayer at high frequencies, ϵ_{∞} , is 7; (iii) the dielectric strength $\Delta\epsilon_2$ is the amplitude of the high-frequency process in eq 2.

In the fractal model (eq 14), R is equal to the size of the Kirkwood cell and R_m is the dimension for one PC molecule dipole (i.e., the radius of the base of the cone). For a hexagonal Kirkwood cell the ratio $R_m/R = 1/3$.

Figure 7 shows the temperature dependencies of the number of defects in a unit cell for PC liposomes without additives, as calculated by using both the classical and fractal models. The best reconciliation of the fractal and classical models was achieved with the geometrical factor Ω being equal to 0.28. Similar values for Ω and ϵ_{∞} were obtained for all other samples with additives, with the exception of the 20 mol % concentration. (This observation was not unexpected because neither model provides for the location of the additive at the bilayer surface. Both models therefore break down at the highest concentration of the additive.) However, at low concentrations of additive and on the scale of the Kirkwood cell, both models are in good agreement.

4.3. Influence of Temperature and Additives on the Structure of the PC Headgroup Region. Through the use of the above models, let us consider the influence of different additives on the mobility of PC bilayer headgroups. It should be mentioned that this influence depends on temperature, and therefore, we have first analyzed the temperature behavior of the dielectric parameters.

As mentioned above, the temperature dependencies of the characteristic frequency of the fast relaxation process demonstrates non-Arrhenius behavior (see Figure 3) and can be well described by the VFT equation:

$$\log f_{\text{fast}} = \log f_0 - \frac{A}{T - T_0} \quad (15)$$

where $\log f_0$ and A are constants. T_0 is the so-called Vogel temperature, which is found to be 30–70 K below the glass transition temperature T_g .¹⁶ The generality of the VFT equation near T_g suggests that T_0 is a significant temperature for the dynamics of glass-forming materials, although the physical meaning of T_0 is not yet clear. There is a well-known correlation between non-Debye and non-Arrhenius temperature behaviors in glass-forming liquids and liquid crystal polymers^{29,30} in which the temperature dependencies of the relaxation rate can be described by the VFT function. In this study, therefore, it is not unexpected that the non-Arrhenius behavior is observed in the PC bilayer.

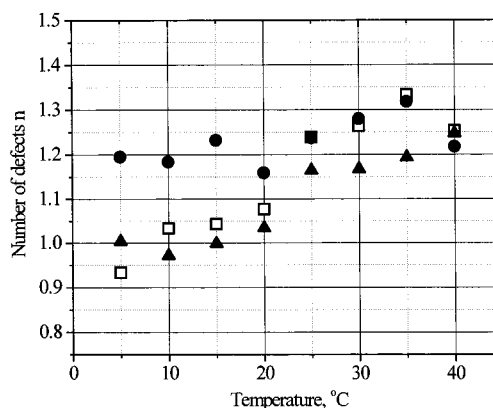


Figure 8. Temperature dependencies of number of defects in the Kirkwood unit cell without additive (□), with 5% of Azone (*), and with 5% of Transcutol (●).

The structure and dynamic state of the bilayer are defined by the interplay of different short and long distance and time scale factors, i.e., hydrophobic forces, dipole–dipole interactions (including hydrogen-bonding), and electrostatic forces. The behavior of the dielectric parameters reflects the general fluidization of the bilayer as the temperature increases. In the temperature interval from 5 to 40 °C the Kirkwood correlation factor g_1 decreases from 3.75 to 2.75 for the pure liposome sample (without additives), indicating that the molecular order in the system is reduced and that the interactions between neighboring dipoles decrease as the temperature increases. The same relationship is usually observed in many pure associated liquids. The temperature dependency of g coincides with the behavior of parameter β , which increases with increasing temperature (Figure 5). In the framework of our models, both observations imply that there is a decrease in the correlation between dipoles and that the distribution of defects in the system becomes more homogeneous. This is confirmed by the temperature dependence of the number of defects (Figure 7). The number of defects increases with increasing temperature, indicating that the permeability of the membrane surface phase may also increase with increasing temperature. It is noted, however, that there is a difference in the behavior of the dielectric parameters between the two kinds of additives.

It is thought that Transcutol does not affect the phase-transition temperature of saturated, single chain length lipids (e.g., DPPC),⁶ and therefore, this penetration enhancer may not exert an effect via changes in bilayer fluidity. Transcutol is instead assumed to behave by simply increasing the solubility of drugs in the lipid bilayer by acting as a cosolvent in its own right.⁷ However, the exact mechanism by which Transcutol effects the molecular dynamics of the headgroup region remains unknown. One can infer from this work that Transcutol exerts a marked effect on the properties of the bilayer surface phase.

Another situation was observed upon studying Azone as the additive. Azone is presumed to be incorporated into the bilayer, with its alkyl chain in the hydrophobic region and the headgroup close to the headgroups of the lipid.³¹ This agent acts by fluidizing the hydrophobic region, and it reduces the diffusional resistance to solute penetration.³²

In this work, the influence of both additive type and additive concentration on the structure and dynamics of the membrane was found to depend on the temperature, i.e., on the state of the bilayer. The typical dependencies of the Kirkwood correlation factor, g_1 , and the number of defects in the Kirkwood unit cell, n , on the concentration of additives are presented in Figures 9 and Figure 10, respectively. In each case, part a represents

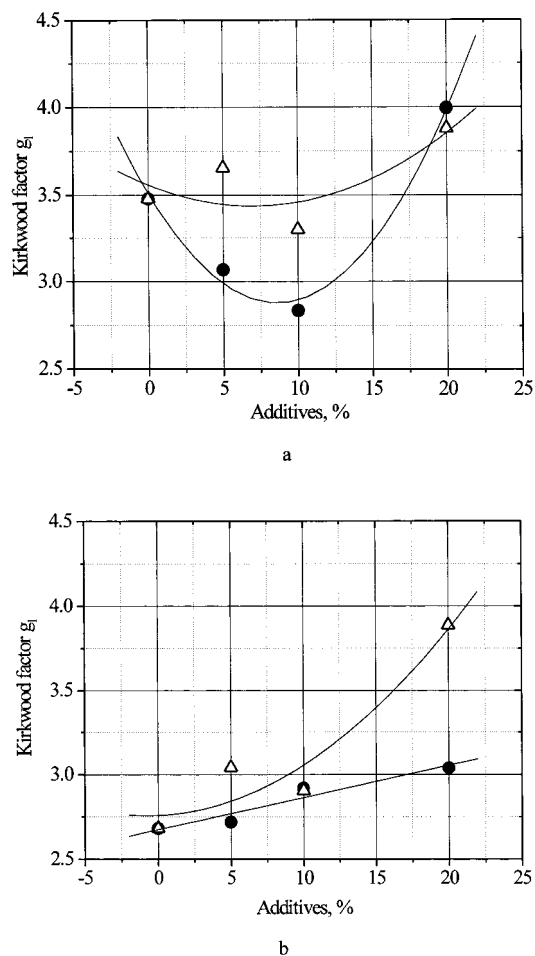


Figure 9. Kirkwood correlation factor g_1 as a dependence of the additive amount at 10 °C (a) and 35 °C (b): (●) with Transcutol additive; (Δ) with Azone additive.

typical data for the low-temperature behavior of the headgroups with increasing additive concentration, and part b represents typical data for the low-temperature behavior of the same.

At high temperatures (i.e., >20 °C), the Kirkwood correlation factor increases with increasing concentration of each additive (Figure 9b) and the number of defects in the unit cell decreases (Figure 10b). The behavior of these parameters is interpreted in terms of the membrane surface becoming more ordered, and therefore, penetration through the surface is likely to decrease at high temperatures. The greatest effect is seen with 20 mol % Azone. We assume that Azone molecules are located close to the interfacial region of the polar headgroups. In this position, this additive exerts a marked effect on the behavior of the headgroups because the large rigid headgroup of Azone can cause a lateral compression in the surface phase of the bilayer, resulting in increased ordering and correlation between headgroups. Transcutol exerts a lesser effect than Azone, probably partly owing to the fact that Transcutol is much more water-soluble than Azone, and therefore, on hydration of the lipid—Transcutol film the majority of the Transcutol partitions into the aqueous phase. The resultant loss of Transcutol from the polar headgroup region may then partly explain why this additive has a minimal effect on the headgroup region.

At low temperatures (i.e., ≤20 °C), the behavior of the Kirkwood correlation factor g_1 (Figure 9a) and the number of defects n in the unit cell (Figure 10a) are more complex than at high temperatures. In the interval from 0 to 10% of Transcutol, the decrease in g and the increase in n both indicate that the

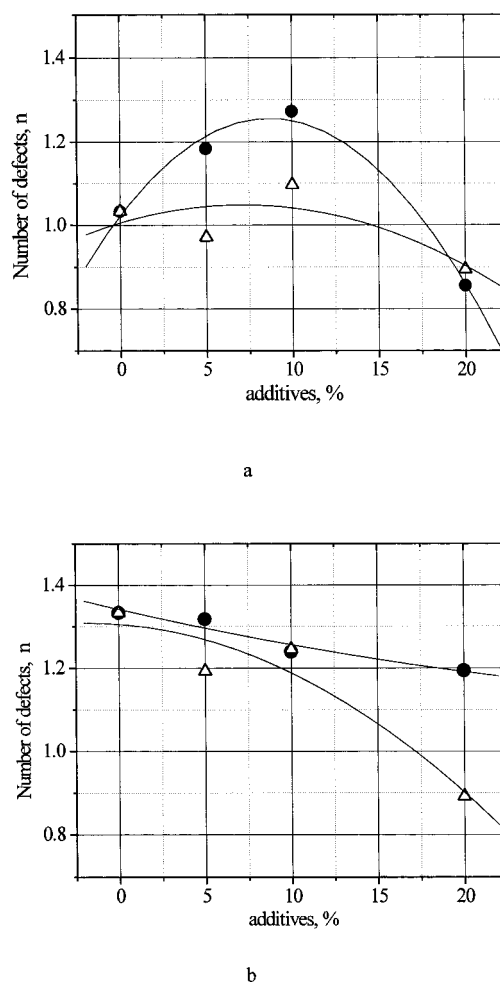


Figure 10. Number of defects in unit cell as a dependence of the additive amount at 10 °C (a) and 35 °C (b): (●) with Transcutol additive; (Δ) with Azone additive.

bilayer becomes more disordered and that increased penetration through the surface phase may therefore follow. In contrast, Azone has little or no effect at these concentrations. It is possible that the pronounced effect from Transcutol results from an increase in the solubility of Transcutol in the headgroup region at low temperatures, thereby fluidizing the environment of the PC headgroups. At 20 mol % of each additive, the behavior of the parameters g_1 and n change sharply, indicating that a degree of order returns to the bilayer. This effect may be explained if there is an increase in the aggregation tendency of additive molecules that then results in some kind of Azone-rich or Transcutol-rich pools in the bilayer surface. This situation may be preferable from the point of view of minimum energy and occurs with a decrease of temperature. The presence of enhancer-rich pools in skin lipid bilayers has been suggested as a potential mode of action for certain enhancers (in particular Azone). These pools may provide an alternative and more permeable pathway for solute diffusion. The presence of Azone or Transcutol pools may then make an impact on the arrangement of the headgroups in the remaining parts of the bilayer. If the presence of additive pools results in the compression of the remainder of the bilayer, then this would give rise to a more ordered system with fewer defects than are present in the bilayer without additive.

V. Conclusions

Analysis of the dielectric relaxation in the polar surface phase of the PC bilayer has shown that the penetration enhancers

Transcutol and Azone exert a marked effect on the dynamic behavior of PC headgroups. The model developed in this paper has allowed the authors to establish the interconnection between the structural and dynamic parameters of the headgroup of PC vesicles and to estimate the number of defects in the Kirkwood unit cell. This number of defects reflects the extent of intermolecular interactions within the bilayer surface and has specific concentration and temperature dependencies for Azone and Transcutol. In terms of the physical modulation of the polar surface phase, it appears that these additives can behave either as enhancers or as retarders. Their activity in this respect depends on the concentration of the additive and the degree of fluidization of bilayer. At high temperatures, both additives manifest retarder-like properties, with Azone exerting the more pronounced effect. At low temperatures (<20 °C) and low concentrations (<20 mol %), Transcutol causes the disruption of the interheadgroup interactions, which may impart enhanced permeability to the membrane surface. The effect of Azone at low temperatures and concentrations, however, is minimal. At 20 mol %, the possible formation of additive pools (again at the low temperatures of the study) may explain the change in effect for both additives at this higher concentration. The mechanism of action of these additives may therefore be a complex function of the modulated properties of the headgroup region of skin lipid bilayers as well as the more usually recognized disruption of the hydrocarbon region.

Acknowledgment. We acknowledge the financial support from the Valazzi-Pikovsky Fellowship Fund (I.E.) and the Eshkol Fellowship Fund (Yu.P.) from the Israel Ministry of Science and Technology. We are grateful also to Prof. Y. Barenholz and Prof. D. Lichtenberg for helpful discussions and to H. Derbyshire for technical assistance.

Appendix

Statistical Fractal Model. This model considers a set of correlation regions that consist of stick correlated defect dipoles. For simplification we assume that all correlation regions have the same shape, but their size, R_s , varies from R_k to R_{\max} , i.e., $R_k < R_s < R_{\max}$. In this case, the spatial nonhomogeneity of defects in the liposome surface can then be described by the volume (area) v of the defect dipole correlation region of size R_k , where $R_s > R_k$:

$$v(R_s, R_k) = v_0(R_k) n(R_s, R_k) \quad (\text{A1})$$

Here,

$$v_0(R_k) = G_{\text{of}} R_k^b \quad (\text{A2})$$

is the volume of the nonhomogeneity on the scale of R_k , G_{of} is the geometric form factor, which takes into account the shape of nonhomogeneity on the scale of R_k , b is the Euclidean dimension of the object (in our case $b = 2$), and

$$n(R_s, R_k) = G_f \left(\frac{R_s}{R_k} \right)^D \quad (\text{A3})$$

is the number of R_k -sized nonhomogeneities in the volume on the scale of R_s . In eq A3, D is the mass fractal dimension of the object, and G_f is the geometric form factor (which depends on both the shape of the considered volume of size R_s and the shape of nonhomogeneity on the scale of R_k). (Note that G_f is the coefficient of proportionality between the area value S and the square of its linear dimension R ; i.e., $G_f = S/R^2$.)

Since the spatial distribution of defects is random in the different realizations of a cell with a size of R_s on the surface of a liposome, then both the minimal size of the correlated area R_k and its geometric shape (i.e., the form factors G_{of} and G_f) will also be random. The volume R_k can vary from R_m , the size of the elementary dipole, up to R_s , the scale of the considered cell.

Taking into account the random character of the spatial defect for the macroscopic description of object, it is necessary to pass from random volume v to its average one $\langle v \rangle$ by statistical averaging of eq A1. For the purpose of simplification, we believe that the random form factors do not depend statistically on the random minimal scale, R_k , and therefore, we obtained

$$\langle v \rangle = G R_s^D \int_{R_m}^{R_s} R_k^{b-D} W(R_k) dR_k \quad (\text{A4})$$

where

$$G = \langle G_{\text{of}} G_f \rangle \quad (\text{A5})$$

is some averaged form factor, $W(R_k)$ is the density of distribution of the random scale R_k probability in the statistical ensemble of different cell realization.

Now we can proceed from the average volume of a non-homogeneity to the average number, $\langle n_i \rangle$, of defects on the scale of R_m in the Kirkwood cell (i.e., when $R_s = R$). Since the volume of one defect is described as

$$v_d = G_d R_m^b \quad (\text{A6})$$

where G_{of} is the geometric form factor of the defect, then an equation for the average number of defects in Kirkwood cell $\langle n_i \rangle$ can be written as

$$\langle n_i \rangle = \frac{\langle v \rangle}{v_d} = \Omega R_m^{-b} R^D \int_{R_m}^R R_k^{b-D} W(R_k) dR_k \quad (\text{A7})$$

where $\Omega = G/G_d$.

Since the type of distribution function is unknown, we therefore took the simplest approximation, i.e., that the distribution of R_k in a specified interval is uniform and is given by

$$W(R_k) = A \quad \text{at } R_m \leq R_k \leq R \quad (\text{A8})$$

where the constant A is defined from the normalization condition

$$\int_{R_m}^R W(R_k) dR_k = 1 \quad (\text{A9})$$

and can be written as

$$A = \frac{1}{R \left(1 - \frac{R_m}{R} \right)} \quad (\text{A10})$$

The integration in eq A7 by using distribution functions A8–A10 gives an expression for the number of defective dipoles in the Kirkwood cell in the framework of the fractal model.

$$\langle n_i \rangle = \Omega \frac{\left(\frac{R_m}{R} \right) \left[1 - \left(\frac{R_m}{R} \right)^{b-D+1} \right]}{1 - \frac{R_m}{R}} \quad (\text{A11})$$

References and Notes

- (1) Schaefer, H.; Redelmeier, T. E. *Skin Barrier. Principles of Percutaneous Absorption*; Karger: Basel, Switzerland, 1996; pp 43–86.

- (2) Walters, K. A.; Hadgraft, J., Eds. *Pharmaceutical Skin Penetration Enhancement*; Marcel Dekker: New York, 1993.
- (3) Goodman, M.; Barry, B. W. *Anal. Proc.* **1986**, 23, 397.
- (4) Mak, V. H. W.; Potts, R. O.; Guy, R. H. *Pharm. Res.* **1990**, 7, 835.
- (5) Gay, C. L.; Murphy, T. M.; Hadgraft, J.; Kellaway, I. W.; Evans, J. C.; Rowlands, C. C. *Int. J. Pharm.* **1989**, 49, 39.
- (6) Watkinson, A. C.; Hadgraft, J.; Bye, A. *Int. J. Pharm.* **1991**, 74, 229.
- (7) Harrison, J. E.; Watkinson, A. C.; Green, D. M.; Hadgraft, J.; Brain, K. R. *Pharm. Res.* **1996**, 13, 542.
- (8) Pottel, R.; Gopel, K.-D.; Henze, R.; Kaatze, U.; Uhlendorf, V. *Biophys. Chem.* **1984**, 19, 233.
- (9) Shepherd, J. C. W.; Buldt, G. *Biochim. Biophys. Acta* **1978**, 514, 83.
- (10) Kaatze, U.; Gopel, K.-D.; Pottel, R. *J. Phys. Chem.* **1985**, 89, 2565.
- (11) Buchet, R. *Chem. Phys. Lipids* **1988**, 4, 299.
- (12) Smith, G.; Shekunov, B. Yu.; Shen, J.; Duffy, A. P.; Anwar, J.; Wakerley, M. G.; Chakrabarti, R. *Pharm. Res.* **1996**, 13, 1181.
- (13) Hadgraft, J.; Guy, R. H., Eds. *Transdermal Drug Delivery*; Marcel Dekker: New York, 1989; pp 1–22.
- (14) Vance, D. E.; Vance, J., Eds. *Biochemistry of Lipids, Lipoproteins and Membranes*; Elsevier: Amsterdam, 1991; Chapter 1.
- (15) Feldman, Yu.; Andrianov, A.; Polygalov, E.; Ermolina, I.; Romanichev, G.; Zuev, Y.; Milgotin, B. *Rev. Sci. Instrum.* **1996**, 67, 3208.
- (16) Schonhals, A.; Kremer, F. *J. Non-Cryst. Solids* **1994**, 172–174, 336.
- (17) Schwan, H. P.; Takashima, S.; Miyamoto, V. K.; Stoeckenius, W. *Biophys. J.* **1970**, 10, 1102–1119.
- (18) Pottel, R.; Kaatze, U.; Muller, St. *Ber. Bunsen-Ges. Phys. Chem.* **1978**, 82, 1086–1093.
- (19) Klosgen, B.; Reichle, C.; Kohlsmann, S.; Kramer, K. D. *Biophys. J.* **1996**, 71, 3251–3260.
- (20) Kaatze, U.; Henze, R.; Pottel, R. *Chem. Phys. Lipids* **1979**, 25, 149–177.
- (21) Takashima, S. *Electrical Properties of Biopolymers and Membranes*; Adam Hilger: Bristol, Philadelphia, 1989; Chapter 2.
- (22) Schwan, H. P. *Adv. Biol. Med. Phys.* **1957**, 5, 147.
- (23) Seelig, J.; Gally, H.-U.; Wohlgemuth, R. *Biochim. Biophys. Acta* **1977**, 467, 109.
- (24) Bottcher, C. J. F. *Theory of Electric Polarization*, 2nd ed.; Elsevier: Amsterdam, 1993; Vol. 1, Chapter VI.
- (25) Raudino, A.; Mauzerall, D. *Biophys. J.* **1986**, 50, 441.
- (26) Pottel, R.; Kaatze, U.; Muller, St. *Ber. Bunsen-Ges. Phys. Chem.* **1978**, 82, 1086.
- (27) Kraszewski, A. *J. Microwave Power* **1977**, 12 (3), 215.
- (28) Nigmatullin, R. R.; Ryabov, Ya. E. *Phys. Solid State* **1997**, 39, 87.
- (29) Richert, R.; Blumen, A., Eds. *Disorder effects on relaxation processes*; Springer-Verlag: Berlin, 1994; Chapter 10.
- (30) Runt, J. P.; Fitzgerald, J. J., Eds. *Dielectric spectroscopy of polymeric materials*; American Chemical Society: Washington, DC, 1996; Chapter 3.
- (31) Hadgraft, J.; Williams, D. G.; Allan, G. In *Pharmaceutical Skin Penetration Enhancement*; Walters, K. A., Hadgraft, J. A., Eds.; Marcel Dekker: New York, 1993; pp 175–197.
- (32) Beastall, J. C.; Hadgraft, J.; Washington, C. *Int. J. Pharm.* **1988**, 43, 207.